Applied Entomology and Zoology (2023) 58:149–160
https://doi.org/10.1007/s13355-023-00816-x

ORIGINAL RESEARCH PAPER

Voltage-gated ion channels in central neurons of *Helicoverpa armigera* as potential targets for cycloxaprid: a *cis*-configuration neonicotinoid insecticide

Xiao Liu[1] · Man Chen[1] · Zheng Ma[1] · Yongchuan Yang[1] · Yangxingzi Li[1] · Hongmei Li-Byarlay[2] · Bingjun He[1]

Received: 1 June 2022 / Accepted: 9 January 2023 / Published online: 19 January 2023

Abstract

Cycloxaprid is a novel *cis*-neonicotinoid, mainly acting on the nicotinic acetylcholine receptor; however, it is not clear whether cycloxaprid can act on voltage-gated ion channels. In this study, the effects of cycloxaprid on the sodium, calcium and potassium channels in central neurons acutely dissociated from *Helicoverpa armigera* Hübner (Lepidoptera: Noctuidae) were investigated by the whole-cell patch clamp technique. With the application of cycloxaprid, the half voltage ($V_{0.5}$) of activation and inactivation of sodium channels exhibited an obvious hyperpolarizing shift around 4–16 mV and 4–14 mV, respectively. The window currents of sodium channels increased by 35.04–88.89%. The time course of recovery from inactivation was also significantly prolonged by 0.25–0.43 ms. The $V_{0.5}$ of activation and inactivation of calcium channels exhibited a marked hyperpolarizing shift around 6–9 mV and 13–19 mV, respectively. The window currents of calcium channels increased by 13.82–28.97%. The time course of recovery from inactivation for calcium channels was prolonged by 0.76–16.85 ms, although not significantly. Comparatively, the peak currents and the $V_{0.5}$ of activation of potassium channels showed no significant change. These results indicate that sodium and calcium channels of *H. armigera* are potential target sites of cycloxaprid.

Keywords Cycloxaprid · *Helicoverpa armigera* · Voltage-gated calcium channel · Voltage-gated potassium channel · Voltage-gated sodium channel

Introduction

The cotton bollworm, *Helicoverpa armigera* (Hübner) (Lepidoptera: Noctuidae), is one of the most severe cosmopolitan agricultural pests (Tian et al. 2021). It is widely distributed in Asia, Africa, Europe, and other regions (Reddy and Manjunatha 2000) and can attack more than 200 wild and crop species, including a range of fruits, vegetable crops, and tree species (Sarate et al. 2012). Although many pest management practices have been implemented, its control depends almost exclusively on insecticides (Wang et al. 2021).

At present, the insecticides occupying the largest market share in the pesticide field globally are neonicotinoids, which mainly act on the nicotinic acetylcholine receptor (nAChR) (Jeschke and Nauen 2008; Jeschke et al. 2011; Ohno et al. 2009). These pesticides have a wide insecticidal spectrum, high insecticidal activity, and environmental friendliness (Casida 2018; Matsuda et al. 2001). Yet because of the excessive usage of neonicotinoids and the lack of alternative pesticides, several species, including the cotton aphid (*Aphis gossypii*) (Shi et al. 2011; Wang et al. 2007), whitefly (*Bemisia tabaci*), brown planthopper (*Nilaparvata lugens*) and peach-potato aphid (*Myzus persicae*) (Bass et al. 2011; Liu et al. 2005), have developed resistance to them.

Ion channels are targets of many pesticides and are strongly correlated with insecticide resistance (Ahmad et al. 1989; Dong 2007). Recent studies have shown that several neonicotinoids can affect sodium, calcium and potassium

Xiao Liu and Man Chen contributed equally to this work.

✉ Bingjun He
hebj@nankai.edu.cn

[1] Key Laboratory of Bioactive Materials, Ministry of Education, College of Life Sciences, Nankai University, Tianjin 300071, China

[2] Agricultural Research and Development Program, Central State University, 1400 Brush Row Road, Wilberforce, OH, USA

channels, which are considered as potential targets for neonicotinoids and are related to insecticide resistance (Guan et al. 2020; Liu et al. 2021). Liu et al. (2021) found that the peak currents of sodium channels and calcium channels of *H. armigera* were significantly inhibited by nitenpyram and that both the half voltage of activation and inactivation of sodium and calcium channels moved in the hyperpolarization direction. In addition, the window currents of sodium and calcium channels were significantly increased. Furthermore, Guan et al. (2020) found that guadipyr could effectively affect the gating properties of calcium and potassium channels.

Cycloxaprid (Cyc) is a novel synthesized neonicotinoid pesticide developed by East China University of Science and Technology (Li and Dewey 2011; Pan et al. 2014; Shao et al. 2011). Structurally, Cyc is the only *cis*-nitromethylene neonicotinoid, the nitro substituent of Cyc is in the *cis*-configuration, but that of all other neonicotinoids (such as imidacloprid, thiamethoxam, acetamiprid, nitenpyram, and guadipyr) is in the *trans*-configuration (Shao et al. 2011). Because of its unique structure, Cyc has insecticidal advantages compared with other pesticides. Field trials have shown that Cyc has a wide insecticidal spectrum (Cui et al. 2012, 2016; Jin et al. 2020), high efficacy, no cross-insecticide resistance (Fang et al. 2018; Shao et al. 2010) and low toxicity to mammals and pollinators (Annely et al. 2016; Cui et al. 2016). However, it is not clear whether Cyc can also act on the sodium, calcium and potassium channels in *H. armigera*. The purpose of this research was to explore, using the whole-cell patch clamp technique, whether the voltage-gated sodium, calcium and potassium channels in the central neurons of *H. armigera* are potential targets for this new type of pesticide, Cyc, to further elucidate its insecticidal mechanism.

Materials and methods

Insect and preparation of acutely dissociated central neurons

The cotton bollworm, *H. armigera* were originally collected from field in Hebei province of China in August of 1992, which were divided into two populations in laboratory. One population was selected for four circulations via single pair elimination method with specific insecticide to gain highly sensitive generations to insecticide as the sensitive strain. The sensitive insects were purchased from Institute of Plant Protection, Academy of Agricultural Science of China in 1997, and was continuously raised indoors without any treatment. The larvae were fed on a semi-artificial diet after cooked thoroughly in laboratory with the following materials: 150 g cornmeal, 50 g soybean meal, 15 g yeast power, 5 g agar powder, 0.5 g sorbic acid, 1.25 g citric acid, 5 g vitamin C, 0.75 g multivitamin, 3 mg erythromycin, and 525 mL distilled water. Adults were fed on a mixture solution of glucose, honey and vitamin E. Both larvae and adults were reared at 27 ± 1 ℃ and at a relative humidity of 65–80% with a 12 h light/12 h dark photoperiod. Additionally, it should be noted that the pupal stage required complete darkness.

The third instar larvae of *H. armigera* were starved for 12 h in advance, and then sterilized in 75% ethanol for 2–3 min and washed 2–3 times with a sterilized insect saline solution composed of (in mM) NaCl (100), KCl (4), $CaCl_2$ (2), $MgCl_2$ (1), Hepes (10), d-mannitol (130) and glucose (5), pH was adjusted to 7.0 with 1 M NaOH (Wu et al. 2021). The dorsal side of the larva was carefully dissected to remove the ventral nerve cord, which was rapidly dropped into the sterilized insect saline solution. In addition, extra fat tissues and the neural sheath of ganglia were removed with homemade stripping needles. The processed ventral nerve cord was incubated in 0.125% trypsin for 8 min, and then transferred to a sterile plastic culture dish filled with about 200 μL culture medium containing (in mg/mL) glucose (0.7), fructose (0.4), succinic acid (0.06), TC-yeast extract (2.8), imidazole (0.06), TC-100 insect medium (1.37), Hepes (10) and lactalbumin hydrolysate (2.8), and then gently dissociated with fire-polished Pasteur pipette (Wu et al. 2021). The isolated neurons were incubated at 27 ± 1 ℃ for 2 h before electrophysiological experiments.

Cycloxaprid was purchased from Dr. Ehrenstorfer GmbH (Augsburg, Germany). It was dissolved in dimethylsulfoxide (DMSO) to obtain a 20 mM stock solution. The stock solution were diluted in extracellular solution to achieve the required concentrations for the electrophysiological experiments. The final concentration of DMSO in extracellular medium did not exceed 0.1%.

Whole-cell patch clamp tests

All experiments were performed at 25 ± 2 ℃. After incubation in the culture medium for approximately 2 h, cells were carefully rinsed 2–3 times with the extracellular solution. Glass microelectrodes were fabricated with P-97 micropipette puller (Sutter Instrument, Novato, CA) and polished with MF-830 micro forge (Narishige Amityville, NY). After being filled with intracellular solution, the patch electrodes had a resistance of 2–3 MΩ. The extracellular solution for recording the sodium currents contained (in mM) NaCl (130), KCl (4), $CaCl_2$ (2), $MgCl_2$ (2), Hepes (10), glucose (10), 4-AP (1, 4-aminopyridine) (5), TEA-Cl (tetraethylammonium chloride) (20) and $CdCl_2$ (0.5), adjusted to pH 6.8 with 1 M NaOH. When necessary, d-tubocurarine chloride pentahydratem (99.50%, Glpbio, Montclair, USA, 10 μM) was added to the extracellular solution for verifying the

absence of nAChRs channel currents. The intracellular solution for recording sodium currents contained (in mM) CsCl (40), CsF (100), $MgCl_2$ (2), EGTA (10) and Hepes (10), adjusted to pH 6.8 with 2 M CsOH. The extracellular solution for recording calcium currents contained (in mM) NaCl (100), CsCl (4), $BaCl_2$ (5), $MgCl_2$ (2), Hepes (10), glucose (5), 4-AP (5), TEA-Cl (20) and 1 µM TTX (tetrodotoxin, Sigma, St. Louis, MO), adjusted to pH 6.8 with 1 M NaOH. The intracellular solution for recording calcium currents contained (in mM) CsCl (120), $MgCl_2$ (2), Na_2-ATP (5), EGTA (11) and Hepes (5), adjusted to pH 6.8 with 2 M CsOH. The extracellular solution for recording potassium currents contained (in mM) NaCl (148), KCl (5), $CaCl_2$ (2), $MgCl_2$ (1), Hepes (10), Glucose (5), $CdCl_2$ (0.5) and 1 µM TTX, adjusted to pH 6.8 with 1 M NaOH. The intracellular solution for recording potassium currents contained (in mM) KCl (150), $MgCl_2$ (2), Na_2-ATP (0.2), EGTA (10) and Hepes (10), adjusted to pH 6.8 with 1 M KOH. The final osmolarity of all solutions were 330–340 mOsm. Whole-cell patch clamp recordings were conducted with an EPC-10 amplifier (HEKA, Lambrecht, Germany) and filtered at 5 kHz. Data acquisition and cell stimulation were performed using PatchMaster software, and leak currents were corrected using the P/4 procedure. Insecticides were applied through a custom-fabricated passive perfusion manifold.

Data were analyzed using the software Clampfit 10.2 (Molecular Devices, San Jose, CA) and Origin 9.0 (OriginLab Corp., Northampton, MA). Statistical analysis were conducted with SPSS 20 software (Statistical Product and Service Solutions, IBM Co., Armonk, NY), and statistical significance was judged via the P-value calculated by one-way analysis of variance. If the *P*-value was < 0.05 compared with the control, it was considered statistically significant.

Results

Verification of the absence of nAChRs channel currents

Nicotinic acetylcholine receptors (nAChRs) are ligand-gated ion channels permeable to sodium, potassium, and calcium ions. In insects, they play a major role in excitatory synaptic transmission and are the primary target site for neonicotinoid insecticides. To detect the presence of nAChRs channel currents, a conventional pulse protocol eliciting sodium currents was employed to examine the effects of TEA-Cl and d-tubocurarine on nAChRs channel currents. TEA-Cl can block both muscle-type and neuronal-type nAChRs currents. D-tubocurarine can also inhibit nAChRs channels. As illustrated in figures in supplementary materials, after the application of TEA-Cl (Fig-S 1) or d-tubocurarine (Fig-S 2), both the amplitude of peak currents and current–voltage curves exhibited no visible difference. The results indicate that no nAChRs current was induced in the patch clamp recordings, the inward currents have not been contaminated by nAChR currents.

Effects of cycloxaprid on sodium channels of H. armigera

Verification of the voltage-gated sodium currents

After the establishment of whole-cell recording mode, the control sodium currents were verified. The currents could be completely inhibited by 1 µM TTX indicating that the recorded currents were induced from TTX-sensitive sodium channels (Fig. 1a).

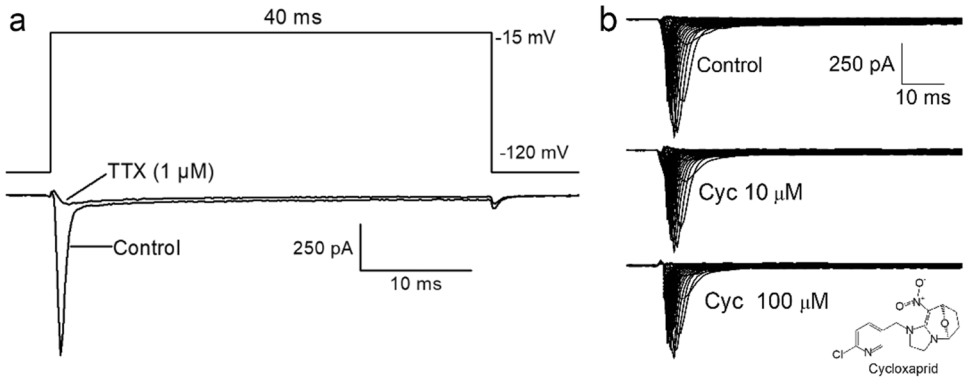

Fig. 1 Effects of tetrodotoxin (TTX) (**a**) and cycloxaprid (Cyc) (**b**) on the voltage-gated sodium channel currents

Table 1 Normalized peak currents of sodium channels before and after the application of cycloxaprid (Cyc)

Condition	Peak currents (pA/pF)[a]	n[b]
Control	− 102.01 ± 7.29	21
Cyc, 0.1 μM	− 97.69 ± 9.23	7
Cyc, 1 μM	− 101.38 ± 12.62	7
Cyc, 10 μM	− 103.72 ± 13.47	8
Cyc, 100 μM	− 117.48 ± 13.42	12

[a]Values are means ± standard errors of separate determinations with different cells and are normalized to the capacitance (in pF) measured for each cell

[b]Number of central neurons applied

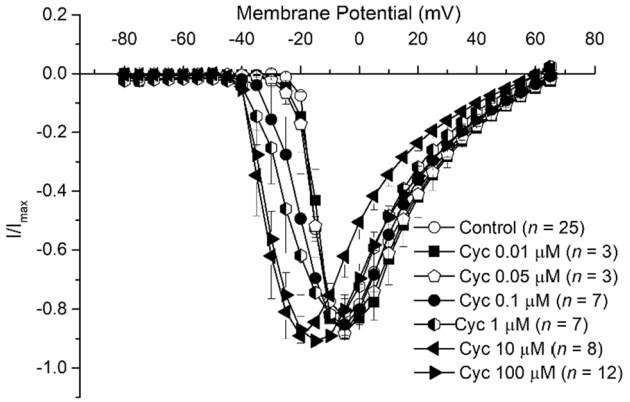

Fig. 2 Current–voltage (I-V) curves of sodium channels before and after the perfusion of Cyc. Points are mean values of all the acquired data. Error bars show standard error values larger than the data point symbols

Effects of cycloxaprid on voltage-dependent activation of sodium channels

Representative whole-cell sodium current traces activated by depolarizing pulses of − 80 mV to 65 mV for 40 ms in 5 mV steps are shown in Fig. 1b. The peak value of sodium currents showed no obvious difference (Table 1), but the current–voltage (I-V) curves showed an obvious hyperpolarizing shift at higher concentration of Cyc (Fig. 2). The sodium currents were activated at approximately − 35 mV and peaked around − 5 mV. Low concentrations of Cyc (0.01 μM and 0.05 μM) had no effect on the I-V curves of sodium channels, but higher concentrations of Cyc shifted the I-V curves toward negative potential approximately 15–20 mV.

The concentration-dependent modification of Cyc on the activation kinetics of sodium channels are illustrated in Fig. 3a, and results of the statistical analysis of these data are summarized in Table 2. Low concentration of 0.1 μM Cyc exhibited visible modification effects on the activation curves of sodium channels. The half activation voltage ($V_{0.5}$) values of sodium channels with the perfusion of 10 μM and 100 μM Cyc were − 32.29 mV and − 30.06 mV, respectively, displaying obvious hyperpolarizing shifts compared with that of − 15.90 mV for the control ($p < 0.05$). A negative shift in the activating potential revealed that sodium channels modified by Cyc could be activated more easily by the depolarizing potentials.

Effects of cycloxaprid on voltage-dependent inactivation of sodium channels

The inactivation curves of sodium channels before and after the infusion of Cyc as well as their statistical significances are exhibited in Fig. 3b and Table 2, respectively. Low

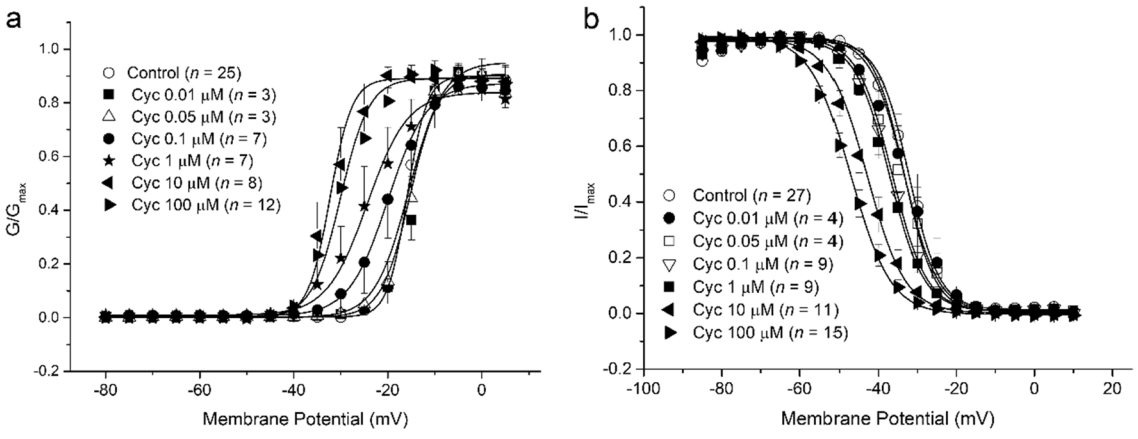

Fig. 3 Concentration-dependent modification of the voltage dependence of activation (**a**) and inactivation (**b**) of sodium channels by Cyc. Points are the mean values of all acquired data. Error bars show standard error values larger than the data point symbols

Table 2 Effects of different concentrations of cycloxaprid (Cys) on the voltage-dependent activation and inactivation of sodium channels

Condition	Activation			Inactivation		
	$V_{0.5}$[a] (mV)	k[b]	n[c]	$V_{0.5}$[d]	k[b]	n[c]
Control	− 15.90 ± 1.04	2.09 ± 0.46	25	− 32.21 ± 0.77	3.93 ± 0.35	27
Cyc, 0.01 μM	− 15.28 ± 0.64	3.04 ± 0.25	3	− 33.41 ± 1.66	4.13 ± 0.49	4
Cyc, 0.05 μM	− 15.49 ± 1.31	3.64 ± 0.38	3	− 33.40 ± 1.34	3.91 ± 0.77	4
Cyc, 0.1 μM	− 19.97 ± 1.34[e]	4.18 ± 0.39[e]	7	− 36.52 ± 0.81[e]	4.44 ± 0.38	9
Cyc, 1 μM	− 24.36 ± 0.64[e]	4.30 ± 0.21[e]	7	− 37.18 ± 0.84[e]	4.43 ± 0.41	9
Cyc, 10 μM	− 32.29 ± 0.78[e]	2.34 ± 0.23	8	− 42.89 ± 0.56[e]	4.87 ± 0.28[e]	11
Cyc, 100 μM	− 30.06 ± 0.72[e]	3.04 ± 0.22[e]	12	− 47.12 ± 0.62[e]	5.13 ± 0.32[e]	15

[a]Half activation voltage for voltage-dependent activation of the sodium channels

[b]Slope factor

[c]Number of central neurons applied

[d]Half inactivation voltage for steady-state inactivation of the sodium channels

[e]Indicates a significant difference compared with the control ($p < 0.05$, one-way analysis of variance)

concentration of 0.1 μM Cyc started to produce visible modification effects on the inactivation curves of sodium channels. The half inactivation voltage ($V_{0.5}$) values of sodium channels infused with 10 and 100 μM Cyc were − 42.89 mV and − 47.12 mV, respectively, showing an obvious hyperpolarizing shift compared with that of − 32.21 mV for the control ($p < 0.05$). Furthermore, the k values of 4.87 and 5.13 for the sodium channels infused with 10 μM and 100 μM Cyc were higher than that of 3.93 for the control ($p < 0.05$; Table 2). These results indicate that the application of Cyc caused the sodium channels to be inactivated more easily.

Effects of cycloxaprid on window current of sodium channels

The sodium window current is the intersection area of the curves for voltage-dependent activation and inactivation, where sodium channels are predicted to spontaneously activate but not completely inactivate. As portrayed in Fig-S 3 in the supplementary materials, the intersectant area increased by 88.89% for 10 μM Cyc (Fig-S 3a) and by 35.04% for 100 μM Cyc (Fig-S 3b) in comparison with the control, revealing that Cyc was able to significantly upregulate the possibility of sodium channels opening under a certain test potential and that the lower concentration of Cyc was more conducive to the opening of sodium channels.

Effects of cycloxaprid on the time course of recovery from the inactivation of sodium channels

The voltage-gated sodium channels could be fully opened in a very short time, and it took several milliseconds for them to recover to the resting state and prepare for the next opening after being inactivated by the depolarization. Figure 4 illustrates the influence of different concentrations of Cyc on the time course of recovery from inactivation

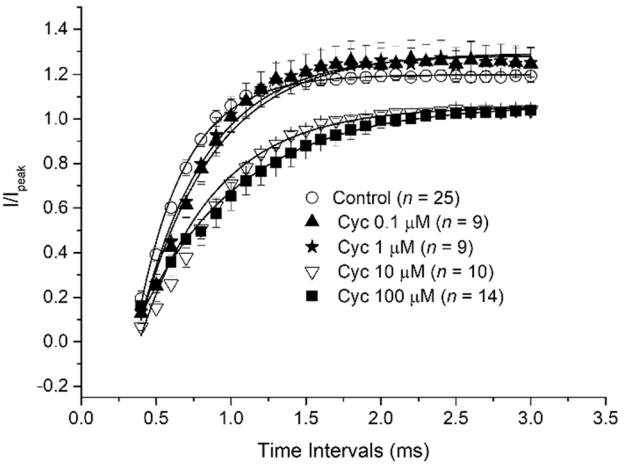

Fig. 4 Effects of Cyc on the time course of recovery from inactivation of sodium channels. The one-phase exponential decay function (ExpDec1) was applied to obtain the curve of recovery from inactivation. Points are the mean values of all acquired data. Error bars show standard error values larger than the data point symbols

of the sodium channels triggered by the double-pulse stimulation. As shown in Table 3, the time course (τ) of sodium channels modified by 10 μM and 100 μM Cyc were elevated by 0.18 ms and 0.35 ms and were statistically significant ($p < 0.05$; Table 3), indicating that Cyc could prolong the time for sodium channels to return to the resting state after inactivation.

Table 3 Effects of cycloxaprid (Cyc) on the time course of recovery from the inactivation of sodium channels

Condition	Recovery from inactivation	
	τ[a]/ms	n[b]
Control	0.32 ± 0.01	25
Cyc, 0.1 μM	0.49 ± 0.03	9
Cyc, 1 μM	0.45 ± 0.03	9
Cyc, 10 μM	0.50 ± 0.01[c]	10
Cyc, 100 μM	0.67 ± 0.02[c]	14

[a]Time course of recovery from inactivation calculated by the one-phase exponential decay function (ExpDec1)

[b]Number of central neurons applied

[c]Indicates a significant difference compared with the control ($p < 0.05$, one-way analysis of variance)

Table 4 Normalized peak currents of calcium channels before and after the application of cycloxaprid (Cyc)

Condition	Peak currents (pA/pF)[a]	n[b]
Control	− 75.29 ± 5.47	16
Cyc, 10 μM	− 51.53 ± 6.96[c]	16
Cyc, 100 μM	− 22.63 ± 4.01[c]	10

[a]Values are means ± standard errors of separate determinations with different cells and are normalized to the capacitance (in pF) measured for each cell

[b]Number of central neurons applied

[c]Indicates a significant difference compared with the control ($p < 0.05$, one-way analysis of variance)

Effects of cycloxaprid on calcium channels of H. armigera

Effects of cycloxaprid on the voltage-dependent activation of calcium channels

Figure 5a depicts a series of representative whole-cell calcium current traces activated by depolarizing pulses of − 80 mV to 65 mV for 300 ms in 5 mV steps, with a holding potential of − 120 mV. The peak currents of the calcium channels modified by Cyc decreased significantly ($p < 0.05$; Table 4), and the I-V curves showed an obvious hyperpolarizing shift comparing with that of the control (Fig. 5b). As portrayed in Fig. 5, the calcium currents for the control were activated at − 40 mV and reached the peak around 0 mV, whereas with the application of Cyc, the I-V curves of the calcium channels moved about 10–15 mV to the negative potential.

The effects of different concentrations of Cyc on the activation kinetics of calcium channels and results of the statistical analysis of these data are displayed in Fig. 6a and Table 5, respectively. With the perfusion of Cyc, the curves of the voltage-dependent activation of calcium channels shifted significantly to the hyperpolarizing direction in a concentration-dependent manner. The $V_{0.5}$ of activation of calcium channels shifted approximately 6.05 and 9.17 mV, respectively, in the hyperpolarizing direction with the application of 10 and 100 μM Cyc (Table 5). A negative shift in the activating potential revealed that calcium channels modified by Cyc were easier to be activated by the depolarizing potentials. Additionally, the *k* values of the activation curves for calcium channels were elevated with the infusion of both 10 and 100 μM Cyc ($p < 0.05$; Table 5).

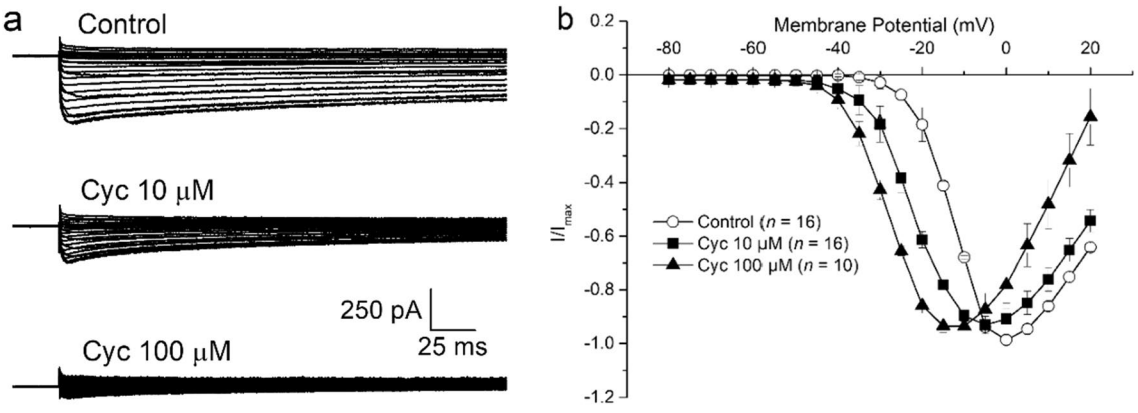

Fig. 5 Representative current traces of the activation of calcium channels before and after the application of Cyc (**a**) and the corresponding current–voltage curves (**b**). Points are the mean values of all acquired data. Error bars show standard error values larger than the data point symbols

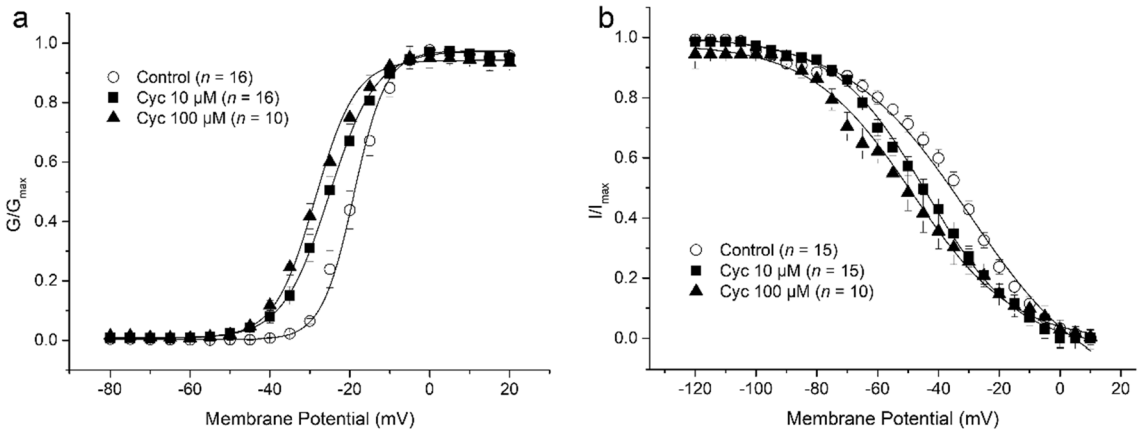

Fig. 6 Modifications of voltage dependence of activation (**a**) and inactivation (**b**) of calcium channels by Cyc. Points are the mean values of all the acquired data. Error bars show standard error values larger than the data point symbols

Table 5 Effects of 10 μM and 100 μM Cyc on the voltage dependence of activation and inactivation of calcium channels

Condition	Activation			Inactivation		
	$V_{0.5}$[a] (mV)	k[b]	n[c]	$V_{0.5}$[d]	k[b]	n[c]
Control	−24.18 ± 0.19	4.62 ± 0.17	16	−31.09 ± 1.15	16.78 ± 0.94	15
Cyc, 10 μM	−30.22 ± 0.18[e]	5.97 ± 0.16[e]	16	−43.68 ± 0.51[e]	16.12 ± 0.50[e]	15
Cyc, 100 μM	−33.35 ± 0.19[e]	5.92 ± 0.16[e]	10	−49.88 ± 1.02[e]	18.63 ± 1.11[e]	10

[a]Half activation voltage for voltage-dependent activation of sodium channels

[b]Slope factor

[c]Number of central neurons applied

[d]Half inactivation voltage for the voltage-dependent inactivation of sodium channels

[e]Indicates a significant difference compared with the control ($p < 0.05$, one-way analysis of variance)

Effects of cycloxaprid on the voltage-dependent inactivation of calcium channels

The inactivation curves of calcium channels before and after the perfusion of Cyc are exhibited in Fig. 6b, and their statistical significances are presented in Table 5. After the application of Cyc, the curves for the voltage-dependent inactivation of calcium channels shifted significantly to the hyperpolarizing direction in a concentration-dependent manner. The $V_{0.5}$ of inactivation moved approximately 12.59 and 18.79 mV in the hyperpolarizing direction by 10 and 100 μM Cyc, respectively (Table 5), and the k value of the inactivation curve for calcium channels with 100 μM Cyc was elevated by 1.85 ($p < 0.05$; Table 5). These results indicate that the application of Cyc caused calcium channels inactivated more easily.

Effects of cycloxaprid on window current of calcium channels

Fig-S 4 in the supplementary materials illustrates the comprehensive effect of the activation and inactivation of

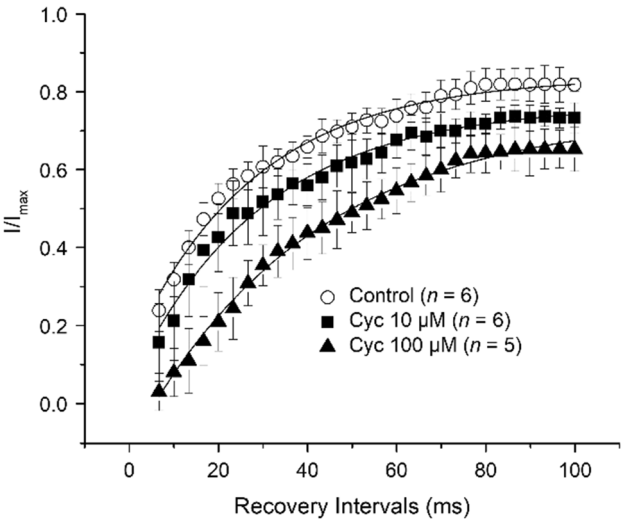

Fig. 7 Effects of Cyc on the time course of recovery from the inactivation of calcium channels. The one-phase exponential decay function (ExpDec1) was applied to obtain the curve of recovery from inactivation. Points are the mean values of all acquired data. Error bars show standard error values larger than the data point symbols

Table 6 Effects of 10 μM and 100 μM cycloxaprid (Cyc) on the time course of recovery from the inactivation of calcium channels

Condition	Recovery from inactivation	
	τ[a]/ms	n[b]
Control	25.25 ± 0.21	6
Cyc, 10 μM	26.01 ± 0.35	6
Cyc, 100 μM	42.10 ± 2.13	5

[a]Time course of recovery from inactivation calculated by the one-phase exponential decay function (ExpDec1)

[b]Number of central neurons applied

calcium channels by Cyc. The intersecting area increased by 13.82% for 10 μM Cyc (Fig-S 4a) and by 28.97% for 100 μM Cyc (Fig-S 4b) in comparison with the control, revealing that the frequency of calcium channel opening under the modification by Cyc was increased in a certain range of membrane potential and that calcium channels not modified by Cyc were inactivated or closed.

Effects of cycloxaprid on the time course of recovery from the inactivation of calcium channels

Figure 7 depicts the influence of Cyc on the time course of recovery from the inactivation of calcium channels. As denoted in Table 6, the time course (τ) of recovery from inactivation was prolonged by approximately 0.76 ms and 16.85 ms by 10 and 100 μM Cyc, respectively, but the results were not statistically significant ($p > 0.05$; Table 6).

Table 7 Normalized peak currents of potassium channels before and after the application of cycloxaprid (Cyc)

Condition	Peak currents (pA/pF)[a]	n[b]
Control	216.42 ± 50.58	10
Cyc, 10 μM	147.72 ± 25.79	8

[a]Values are means ± standard errors of separate determinations with different cells and are normalized to the capacitance (in pF) measured for each cell

[b]Number of central neurons applied

Effects of cycloxaprid on potassium channels of H. armigera

Effects of cycloxaprid on current–potential curves of the potassium channels

Representative whole-cell potassium current traces activated by depolarizing pulses of − 80 mV to 60 mV for 60 ms are shown in Fig. 8a and current–voltage curves of potassium channels with the perfusion of Cyc are portrayed in Fig. 8b. As shown in Fig. 8b, the I-V curve of potassium channels was activated at approximately − 70 mV. However, compared with the control, the I-V curve of potassium channels modified by 10 μM Cyc moved up under the stimulation of a depolarization pulse of approximately − 70 to 30 mV and moved down under the stimulation of a depolarization pulse of approximately 30–60 mV. Furthermore, the peak currents of potassium channels with perfusion of Cyc showed no statistical difference ($p > 0.05$; Table 7).

Effects of cycloxaprid on the voltage-dependent activation of potassium channels

The effects of Cyc on the activation kinetics of potassium channels are illustrated in Fig. 9, and results of the statistical analysis of these data are presented in Table 8. Figure 9

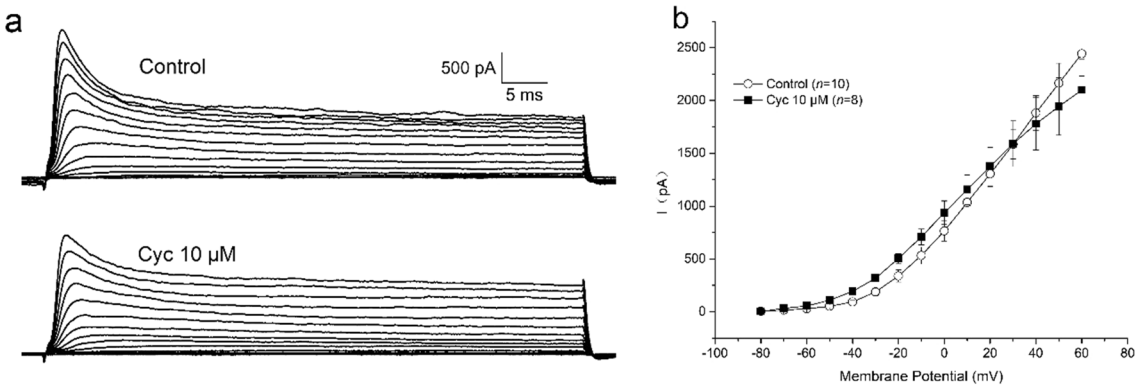

Fig. 8 Representative current traces of activation of potassium channels before and after the application of Cyc (**a**) and the corresponding current–voltage curves (**b**). Points are the mean values of all acquired data. Error bars show standard error values larger than the data point symbols

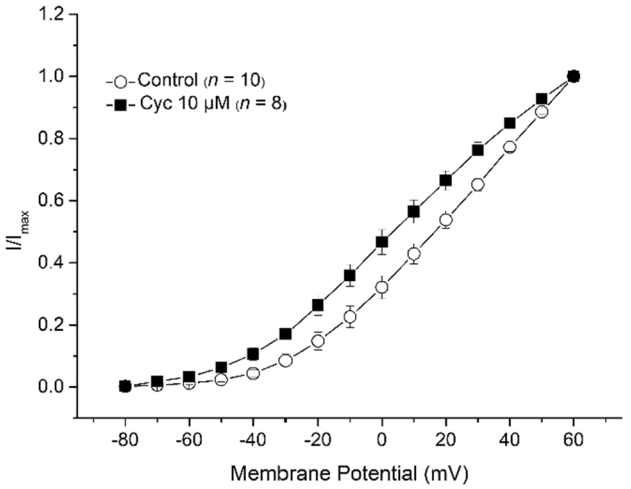

Fig. 9 Modifications of voltage dependence of activation of potassium channels by Cyc. All points are the mean values of all acquired data. Bars show SE values larger than the data point symbols

Table 8 Effects of 10 μM cycloxaprid (Cyc) on the voltage-dependent activation of potassium channels

Condition	Activation		
	$V_{0.5}$[a]	k[b]	n[c]
Control	23.55 ± 3.18	24.95 ± 3.18	10
Cyc, 10 μM	18.62 ± 10.18	31.20 ± 4.44	8

[a]Half activation voltage for the voltage-dependent activation of sodium channels

[b]Slope factor

[c]Number of central neurons applied

illustrates that with the perfusion of Cyc, the $V_{0.5}$ of activation of potassium channels shifted by approximately 4.93 mV in the hyperpolarization direction, but the change was not statistically significant. The k value declined slightly ($p > 0.05$; Table 8).

Discussion

Cycloxaprid is a novel synthesized neonicotinoid pesticide (Li and Dewey 2011; Pan 2014; Shao et al. 2011), and structurally, Cyc is the first *cis*-neonicotinoid insecticide. Laboratory and field experiments have revealed that Cyc had higher toxicity compared with other *trans*-neonicotinoid insecticides against *Erythroneura apicalis* (Homoptera) nympha, *Aphis gossypii* adults, *Bemisia tabaci* adults and *Aorea scutellaris* (Coleoptera) (Tan 2019). Especially, the insecticidal activity of Cyc against resistant brown planthopper was 50 times than that of imidacloprid, a leading *trans*-neonicotinoid insecticide (Shao et al. 2010).

Neonicotinoids mainly act on nAChRs, however, we found that *trans*-neonicotinoids could also affect the sodium, calcium and potassium channels (Guan et al. 2020; Liu et al. 2021). To the best of our knowledge, whether Cyc, as the only *cis*-neonicotinoid, can also act on the sodium, calcium and potassium channels in *H. armigera* is unknown. In this study, the effects of Cyc on voltage-gated sodium, calcium and potassium channels were investigated by the whole-cell patch clamp technique. Obvious differences in the gating kinetics of sodium and calcium channels perfused with Cyc were observed in terms of activation, inactivation and recovery from rapid inactivation. Collectively, our results present clear evidence that Cyc profoundly altered the kinetics of sodium and calcium channels.

Effects of cycloxaprid on sodium channels of H. armigera

Plenty of papers have demonstrated that sodium channels are the principal target of pyrethroids (Bloomquist 1996; Narahashi 2000; Soderlund 2012), and the action of pyrethroids on sodium channels can be characterized by slowing inactivation during a depolarizing pulse and delaying deactivation (Soderlund 2012), causing hyperexcitability in the nervous system (Magby and Richardson 2017; Motomura and Narahashi 2001; He and Soderlund 2011). Although pyrethroids and neonicotinoids have different structures, our previous results indicated that nitenpyram (a *trans*-neonicotinoid) could also shift the curves of voltage-dependent activation and inactivation of sodium channels in the hyperpolarizing direction and effectively inhibit the peak currents of sodium channels of *H. armigera* (Liu et al. 2021), which is consistent with the results of pyrethroids. Similarly, our results indicated that Cyc induced hyperpolarizing shifts in the voltage dependence of sodium channel activation and steady-state inactivation, but had no effect on the peak currents of sodium channels. This might be related to the unique *cis*-configuration of Cyc compared with the *trans*-configuration of nitenpyram. The area under the intersection of the curves for the voltage-dependent activation and inactivation is the window current, reflecting the opening frequency of the channels. Our data indicated that Cyc could cause an increase in the magnitude of the window currents. This means that Cyc could increase the probability of channel opening across a wide range of membrane potentials. Wu et al. (2018) explained that the time course of recovery from inactivation was markedly extended by pesticides, which was related to the modified sodium channels becoming insensitive to the change of membrane potential, and our results were quite consistent with theirs. Collectively, the rates of both activation and inactivation of sodium channels exposed to Cyc became quicker, indicating that the excitatory cycle of neurons decreased and *H. armigera* might be affected from the constant

tremor, sodium channels of *H. armigera* are a potential target for Cyc.

Effects of cycloxaprid on calcium channels of H. armigera

The calcium channels of neuronal cell membrane were found to be potential targets for insecticides, which may contribute to enhancing the toxicity of the insecticide (Breckenridge et al. 2009). Our previous data demonstrated that guadipyr, having both neonicotinoid and semicarbazone insecticidal activities, could shift the curves of voltage-dependent activation and inactivation for calcium channels in the hyperpolarizing direction and could effectively inhibit the peak currents of sodium channels of *H. armigera* in a concentration-dependent manner (Guan et al. 2020). In this study, the peak currents of calcium channels decreased significantly and the I-V curves showed an obvious hyperpolarizing shift in a concentration-dependent manner. Additionally, the marked hyperpolarizing shifts of voltage-dependent activation and inactivation of calcium channels by Cyc were observed to fall into a concentration-dependent pattern, which is quite consistent with the action mechanism of guadipyr on calcium channels. Synthetically, we analyzed the activation and inactivation of calcium channels using the window current, and the results of the increased window current area of calcium channels modified by Cyc were consistent with the modification of guadipyr. Furthermore, we analyzed the time course of recovery from the inactivation of calcium channels with the infusion of Cyc. However, the "run-down" phenomenon of the calcium current (I_{Ca}) in whole-cell patch clamp recording is common, and because the recording time is prolonged, the I_{Ca} would be attenuated to different degrees (Lu et al. 2019). Our results showed that the time course of recovery from the inactivation of calcium channels was significantly extended by Cyc in a concentration-dependent pattern, which was probably affected by I_{Ca} run-down.

In summary, our results indicate that calcium channels are potential target for Cyc. However, whether pesticides affect calcium channels directly or indirectly remains inconclusive. Symington and Clark (2004) demonstrated that deltamethrin could act directly on voltage-gated calcium channels ($Ca_v2.2$), but Han et al. (2015) speculated that pyrethroids might first act on voltage-gated sodium channels of *H. armigera* and then trigger Na^+ influx, causing the cell membranes to continuously depolarize to activate voltage-gated calcium channels. Specific conclusions still need to be verified by experiments.

Effects of cycloxaprid on potassium channels of H. armigera

Voltage-gated potassium channels play an important role in regulating neuronal excitability and other physiological functions, and gating characteristics of potassium channels could be affected by pesticides (Fu et al. 2007). Liu et al. (1990), Wang et al. (2006) studied the modulation of cypermethrin on sodium and potassium channels in the neurons of *Periplaneta fulginosa* by means of voltage clamp technique. They found that cypermethrin could block potassium channels and reduce the peak value of the potassium currents. Guan et al. (2020) explained that guadipyr could change the half activation voltage of the potassium channels of *H. armigera* and shift it to a depolarization position, causing the potassium channels to become activated at a higher potential. However, our results showed a hyperpolarizing shift of the voltage-dependent activation of potassium channels of *H. armigera* with 10 μM Cyc, and although the peak currents of potassium channels decreased with the infusion of 10 μM Cyc, the changes were not statistically significant. This result may be related to the structure of Cyc, which also suggests that Cyc has a smaller effect on potassium channels of *H. armigera.*

Regarding the insecticidal mechanism, we demonstrated that Cyc could influence the activation and inactivation kinetics of sodium and calcium channels, and inhibited the peak currents of calcium channels effectively. Voltage-gated sodium, calcium and potassium channels form the functional basis for the generation and propagation of action potentials in neurons. The sodium and calcium channels conduct inward currents, potassium channels conduct outward currents. The opening of sodium and calcium channels results in the depolarization of cells, and promotes the excitability of cells. The opening of potassium channels hyperpolarizes the cells, leads the cells to a resting state. Cyc inhibited the peak currents of calcium channels, caused an obvious hyperpolarizing shift of inactivation for both sodium and calcium channels, but exhibited little or no effect on potassium channels under experimental conditions. This indicates that Cyc may undergo more extensive modification in the open state of sodium and calcium channels, accelerating the inactivation process of these two kinds of channels, has no effect on outward channels.

Supplementary Information The online version contains supplementary material available at https://doi.org/10.1007/s13355-023-00816-x.

Acknowledgements This work was supported by grants from National Natural Science Foundation of China (Grant number 31871992 and 31371974).

Data availability The data supporting the findings of this study are available within the article and its supplementary materials.

Declarations

Conflict of interest All authors have read and approved the manuscript, and there is no conflict of interest in regard to the research, authorship, and publication of this article.

References

Ahmad M, Gladwell RT, McCaffery AR (1989) Decreased nerve sensitivity is a mechanism of resistance in a pyrethroid resistant strain of *Heliothis armigera* from Thailand. Pestic Biochem Physiol 35:165–171

Annely B, Anna G, Reinhold S, Marina M, Ralph B (2016) The neonicotinoids thiacloprid, imidacloprid, and clothianidin affect the immunocompetence of honey bees (*Apis mellifera* L.). J Insect Physiol 86:40–47

Bass C, Puinean AM, Andrews M, Cutler P, Daniels M, Elias J, Paul VL, Crossthwaite AJ, Denholm L, Field LM, Foster SP, Lind R, Williamson MS, Slater R (2011) Mutation of a nicotinic acetylcholine receptor β subunit is associated with resistance to neonicotinoid insecticides in the aphid *Myzus persicae*. BMC Neurosci 1:12–51

Bloomquist JR (1996) Ion channels as targets for insecticides. Annu Rev Entomol 41:163–190

Breckenridge CB, Holden L, Sturgess N, Weiner M, Sheets L, Sargent D, Soderlund DM, Jin-Sung C, Symington S, Clark JM, Burr S, Ray D (2009) Evidence for a separate mechanism of toxicity for the type I and the type II pyrethroid insecticides. Neuro Toxicology 30:17–31

Casida JE (2018) Neonicotinoids and other insect nicotinic receptor competitive modulators: progress and prospects. Annu Rev Entomol 63:125–144

Cui L, Sun LN, Yang DB, Yan XJ, Yuan HZ (2012) Effects of cycloxaprid, a novel *cis*-nitromethylene neonicotinoid insecticide, on the feeding behavior of *Sitobion avenae*. Pest Manag Sci 68:1484–1491

Cui L, Sun LN, Yang DB, Yan XJ, Yuan HZ (2016) Cycloxaprid: a novel *cis*-nitromethylene neonicotinoid insecticide to control imidacloprid-resistant cotton aphid (*Aphis gossypii*). Pestic Biochem Physiol 132:96–101

Dong K (2007) Insect sodium channels and insecticide resistance. Invertebr Neurosci 7:17–30

Fang Y, Xie P, Dong CH, Han YQ, Tang T, Liu Y, Zhong J, Bai LY, Zhou XM (2018) Cross-resistance and baseline susceptibility of brown planthopper *Nilaparvata lugens* (Hemiptera: Delphacidae) from China to cycloxaprid. J Econ Entomol 111:2359–2363

Fu ZY, Du CY, Yao Y, Liu CW, Tian YT, He BJ, Zhang T, Yang Z (2007) Effects of β-cypermethrin on voltage-gated potassium channels in rat hippocampal CA3 neurons. Acta Phytophysiol Sin 59:63–70 ((**in Chinese with English abstract**))

Guan DY, Jiang XW, Li QY, Liu X, Ma YQ, Chen Q, Chen Q, Li-Byarlay H, He BJ (2020) Effects of guadipyr on voltage-gated calcium and potassium channels in central neurons of *Helicoverpa armigera*. Chin J Appl Entomol 4:841–849 ((**in Chinese with English abstract**))

Han LX, Wu GY, Zang YY, He BJ (2015) Effects of tefluthrin and deltamethrin on intracellular calcium concentration in central neurons of *Helicoverpa armigera*. J Tianjin Norm Univ Nat Sci Ed 35:96–101 ((**in Chinese with English abstract**))

He BJ, Soderlund DM (2011) Differential state-dependent modification of rat $Na_v1.6$ sodium channels expressed in human embryonic kidney (HEK293) cells by the pyrethroid insecticides tefluthrin and deltamethrin. Toxicol Appl Pharmacol 257:377–387

Jeschke P, Nauen R (2008) Neonicotinoids-from zero to hero in insecticide chemistry. Pest Manag Sci 64:1084–1098

Jeschke P, Nauen R, Schindler M, Elbert A (2011) Overview of the status and global strategy for neonicotinoids. J Agric Food Chem 59:2897–2908

Jin JX, Ye ZC, Jin DC, Li FL, Li WH, Cheng Y, Zhou YH (2020) Changes in transcriptome and gene expression in *Sogatella furcifera* (Hemiptera: Delphacidae) in response to Cycloxaprid. J Econ Entomol 114:284–297

Li B, Dewey CN (2011) RSEM: accurate transcript quantification from RNA-Seq data with or without a reference genome. BMC Bioinf 12:1–16

Liu AX, Ning QJ, Chen XL, Huang RQ, Chen ST (1990) Modified action of cypermethrin enantiomers on axonal sodium and potassium channels of *Periplaneta fulginosa* (Serville). Acta Entomol Sin 1:1–6 ((**in Chinese with English abstract**))

Liu ZW, Williamson MS, Lansdell SJ, Denholm I, Han ZJ, Millar NS (2005) A nicotinic acetylcholine receptor mutation conferring target-site resistance to imidacloprid in *Nilaparvata lugens* (brown planthopper). Proc Natl Acad Sci USA 102:8420–8425

Liu Y, Li QY, Liu X, Yang YC, He BJ, Li CS, Ma YQ (2021) Effects of nitenpyram on sodium and calcium channels in the central neurons of *Helicoverpa armigera*. Acta Sci Nat Univ Nankaiensis 54:23–29 ((**in Chinese with English abstract**))

Lu J, Liu Y, Wang TT, Rui CH, He BJ (2019) Effects of cyhalothrin on high voltage activated calcium channels in central neurons of *Helicoverpa armigera*. Acta Sci Nat Univ Nankaiensis 2:44–50 ((**in Chinese with English abstract**))

Magby JP, Richardson JR (2017) Developmental pyrethroid exposure causes longterm decreases of neuronal sodium channel expression. Neurotoxicology 60:274–279

Matsuda K, Buckingham SD, Kleier D, Rauh JJ, Grauso M, Sattelle DB (2001) Neonicotinoids: insecticides acting on insect nicotinic acetylcholine receptors. Trends Pharmacol Sci 22:573–580

Motomura H, Narahashi T (2001) Interaction of tetramethrin and deltamethrin at the single sodium channel in rat hippocampal neurons. Neurotoxicology 22:329–339

Narahashi T (2000) Neuroreceptors and ion channels as the basis for drug action: past, present, and future. J Pharmacol Exp Ther 294:1–26

Ohno I, Tomizawa M, Durkin KA, Naruse Y, Casida JE, Kagabu S (2009) Molecular features of neonicotinoids pharmacophore variants interacting with the insect nicotinic receptor. Chem Res Toxicol 22:476–482

Pan HS, Liu YQ, Liu B, Lu YH, Xu XY, Qian XH, Wu KM, Desneux N (2014) Lethal and sublethal effects of cycloxaprid, a novel *cis*-nitromethylene neonicotinoid insecticide, on the mirid bug *Apolygus lucorum*. J Pest Sci 87:731–738

Reddy GVP, Manjunatha M (2000) Laboratory and field studies on the integrated pest management of *Helicoverpa armigera* (Hübner) in cotton, based on pheromone trap catch threshold level. J Appl Entomol 124:213–221

Sarate PJ, Tamhane VA, Kotkar HM, Ratnakaran N, Susan N, Gupta VS, Giri AP (2012) Developmental and digestive flexibilities in the midgut of a polyphagous pest, the cotton bollworm, *Helicoverpa armigera*. J Insect Sci 12:1–16

Shao XS, Fu H, Xu XY, Xu XL, Liu ZW, Li Z, Qian XH (2010) Divalent and oxabridged neonicotinoids constructed by dialdehydes and nitromethylene analogues of imidacloprid: design, synthesis, crystal structure, and insecticidal activities. J Agric Food Chem 58:2696–2702

Shao XS, Lee PW, Liu ZW, Xu XY, Li Z, Qian XH (2011) *Cis*-configuration: A new tactic/rationale for neonicotinoid molecular design. J Agric Food Chem 59:2943–2949

Shi XB, Jiang LL, Wang HY, Qiao K, Wang D, Wang KY (2011) Toxicities and sublethal effects of seven neonicotinoid insecticides on survival, growth and reproduction of imidacloprid-resistant cotton aphid, *Aphis gossypii*. Pest Manag Sci 67:1528–1533

Soderlund DM (2012) Molecular mechanisms of pyrethroid insecticide neurotoxicity: recent advances. Arch Toxicol 86:165–181

Symington SB, Clark JM (2004) Action of deltamethrin on n-type (Ca_v 2.2) voltage-sensitive calcium channels in rat brain. Pestic Biochem Physiol 82:1–15

Tan HJ (2019) New neonicotinoid insecticide cycloxpyrid and its development. World Pestic 41:59–64

Tian K, Feng J, Zhu J, Cheng JG, Li M, Qiu XH (2021) Pyrethrin-resembling pyrethroids are metabolized more readily than heavily modified ones by CYP9As from *Helicoverpa armigera*. Pestic Biochem Physiol. https://doi.org/10.1016/j.pestbp.2021.104871

Wang Y, He BJ, Zhao Q, Liang Z, Liu AX (2006) Effects of cyhalothrin on the transient outward potassium current in central neurons of *Helicoverpa armigera*. Insect Sci 13:13–17

Wang KY, Guo QL, Xia XM, Wang HY, Liu TX (2007) Resistance of *Aphis gossypii* (Homoptera: Aphididae) to selected insecticides on cotton from five cotton production regions in Shandong, China. J Pest Sci 32:372–378

Wang QQ, Rui CH, Wang L, Nahiyoon SA, Huang WL, Zhu JS, Ji XJ, Yang QJ, Yuan HZ, Li C (2021) Field-evolved resistance to 11 insecticides and the mechanisms involved in *Helicoverpa armigera* (Lepidoptera: Noctuidae). Pest Manag Sci 77:5086–5095

Wu GY, Li L, Chen B, Chen C, Luo DQ, He BJ (2018) Natural meroterpenoids isolated from the plant pathogenic fungus *Verticillium albo-atrum* with noteworthy modification action against voltage-gated sodium channels of central neurons of *Helicoverpa armigera*. Pestic Biochem Physiol 144:91–99

Wu GY, Li QY, Liu X, Li BHM, He BJ (2021) Differential state-dependent effects of deltamethrin and tefluthrin on sodium channels in central neurons of *Helicoverpa armigera*. Pestic Biochem Physiol. https://doi.org/10.1016/J.PESTBP.2021.104836